

Supporting Information

Engineering tough, highly compressible, biodegradable hydrogels by tuning the network architecture

Dunyin Gu, Shereen Tan, Chenglong Xu, Andrea J. O'Connor and Greg G. Qiao*

Department of Chemical and Biomolecular Engineering, The University of Melbourne, Parkville, Victoria 3010, Australia. *Author to whom correspondence should be addressed (gregghq@unimelb.edu.au)

Experimental

Materials

α , ω -dihydroxyl poly(ethylene glycol) (PEG_{6k}; $M_n=6.0 \times 10^3$ Da; PDI=1.02) and α , ω -dihydroxyl poly(ethylene glycol) (PEG_{10k}; $M_n=1.0 \times 10^4$ Da; PDI=1.03) were purchased from Sigma-Aldrich; 4-arm maleimide-poly(ethylene glycol) (4-arm MAL-PEG; $M_n=1.0 \times 10^4$ Da; PDI=1.02) and α , ω -dithiol poly(ethylene glycol) (SH-PEG-SH; $M_n=5.0 \times 10^3$ Da; PDI=1.02) were purchased from Jenkem Technology USA Inc. Methanesulfonic acid (MSA, 98%). Tetrahydrofuran (THF, RCI Labscan, HPLC) was distilled from sodium benzophenone ketyl before use. Toluene (Scharlau, HPLC), dichloromethane (DCM, 99.8%, Merck), ϵ -caprolactone (99+%, Aldrich) and ethyl ether (DEE, 99.8%, Merck) were distilled from calcium hydride (95%, Aldrich) before use. α , ω -dihydroxy poly(ϵ -caprolactone) (PCL_{3k}; $M_n=3.3 \times 10^3$ Da, PDI=1.05) was synthesized according to a previously published procedure.¹ BOD was synthesized according to a previously published procedure.² Doxorubicin hydrochloride was purchased from Sigma-Aldrich and deprotonated with hydroxide sodium solution to form water insoluble doxorubicin. Phosphate buffered saline (PBS) with pH of 7.4 was prepared by using PBS tablets purchased from Sigma-Aldrich. Cell culture supplies (Dulbecco's Modified Eagle Medium (DMEM), Fetal Bovin Serum (FBS), 100 \times GlutaMax, 100 \times antibiotic-antimycotic), AlamarBlue(R) assay reagent were purchased from Life Technologies and used as received.

Characterization and Instrumentation

¹H NMR spectroscopic analysis was performed on a Varian Unity Plus 400 MHz spectrometer using the deuterated solvent as reference. Gel permeation chromatography (GPC) was performed on a Shimadzu liquid chromatography system fitted with a Wyatt OPTILAB DSP interferometric refractometer (690 nm), using three Phenomenex Phenogel columns (500, 104, and 106 Å porosity; 5 μ m-diameter bead size) operated at 1 mL/min using THF as the mobile phase and with the column temperature set at 45 °C. ATR-IR spectroscopy was carried out using a Bruker Tensor 27 FTIR, with GladiATR ATR attachment obtained from Pike Technologies. The FTIR was equipped with OPUS 6.5 spectroscopy software from Bruker Optik GmbH. XRD spectroscopy was carried out on a Bruker D8 Advance Diffractometer, using standard Ni-filtered Cu α radiation. The sample for AFM measurement was prepared by spin-coating a silicon wafer with a 10% (w/v) gel precursor solution at 4500 rpm and drying the wafer in vacuo at 65 °C overnight. The imaging was performed on Dimension Icon AFM system (Bruker, USA) using PeakForce Quantitative Nanomechanical property mapping. The AFM probe (TESPA-V2, Bruker AFM probes) was calibrated on a fresh cleaned sapphire substrate to calculate the deflection sensitivity, and the spring constant is 40N/m determined by the thermal tune method. The sample for STEM/TEM analysis was prepared by cutting a thin cross section of the gel film spin-coated on silicon wafer using Focus Ion Beam (FIB) technology. The sample was visualized on Tecnai F30 (FEI) running at 300kV. Mechanical testing was conducted using an Instron Microtester 5848 equipped with a 2 kN static load cell and Bluehill material testing software. Differential scanning calorimetry (DSC) was performed on a TA Instruments model 2920 modulated DSC under nitrogen flow. DSC calibration was performed using certified indium and sapphire. The dried hydrogel sample was heated from -70 to 150 °C at a heating rate of 20 °C·min⁻¹, then cooled to -70 °C at a cooling rate of 20 °C·min⁻¹. UV-Vis spectrometric analysis was performed using a Shimadzu UV-2101 PC UV-Vis scanning spectrophotometer at a scan rate of 1 nm/s, with paired quartz cuvettes (Starna Pty Ltd).

Preparation of PEG hydrogels

PEG hydrogel was formed by mixing aqueous solutions of 4-arm MAL-PEG-MAL (50 mg, 0.005 mmol, 1 equiv.) and SH-PEG-SH (50 mg, 0.01 mmol, 2 equiv.) in a cylindrical mold, with the total volume of gel precursor solution being 1mL.

Preparation of PEG_{6k}/P(BOD) (EG/CL(BOD)=88/12) hydrogels

PEG/P(BOD) hydrogels were synthesized in one pot via one-step ROP, using PEG as initiator and BOD as cross-linker. Variation of the EG/CL ratio and PEG length can result in different hydrophilic/hydrophobic balance and mechanical properties. In a typical synthesis: the mixture of PEG_{6k} (74.7 mg, 0.012 mmol, 1 equiv.) and BOD (25.3 mg, 0.11 mmol, 9 equiv.) was azeotropically dried in vacuo with toluene followed by back purging with Argon for three times prior to use. Then dry DCM (1 mL) was added via syringe under Argon atmosphere to dissolve them, followed by addition of MSA (2.4 μ L, 0.036 mmol, 3 equiv.) with stirring. The precursor solution mixture was transferred to a cylindrical mold and allowed to stand at room temperature for 24 hours with occasional agitation. The cured gel was removed from the mold and washed with excess THF for three times to remove remaining catalyst and DCM. The resultant gel was immersed in deionized water, which was replaced with fresh water regularly until equilibrium swelling was reached.

Preparation of PCL_{3k}/PEG_{6k}/ P(BOD) (EG/CL(PCL+BOD)=64/36) hydrogels

PCL/PEG/BOD hydrogel was also synthesized in one pot via one-step ROP, using both PEG and PCL as initiators, and BOD as cross-linker. In a typical synthesis: the mixture of PEG_{6k} (40.4 mg, 6.7×10^{-3} mmol, 1 equiv.), PCL_{3k} (23.1mg, 7.7×10^{-3} mmol 1 equiv.), and BOD (36.5 mg, 0.11 mmol, 24 equiv.) was azeotropically dried in vacuo with toluene followed by back purging with Argon for three times prior to use. Then dry DCM (1 mL) was added via syringe under Argon atmosphere to dissolve them, followed by addition of MSA (2.4 μ L, 0.036 mmol, 3 equiv.) with stirring. The precursor solution mixture was transferred to a cylindrical mold and allowed to stand at room temperature for 24 hours with occasional agitation. The cured gel was removed from the mold and washed with excess THF for three times to remove remaining catalyst and DCM. The resultant gel was immersed in deionized water, which was replaced with fresh water regularly until equilibrium swelling was reached.

Preparation of PCL_{3k}-PEG_{10k}-PCL_{3k}/P(BOD) (EG/CL(PCL+BOD)=64/36) hydrogels

PCL-PEG-PCL/P(BOD) hydrogels were synthesized in one pot yet via two-step ROP, with addition of ϵ -caprolactone to convert PEG to macroinitiator, PCL-PEG-PCL. In a typical synthesis: PEG_{10k} (40.4 mg, 4.0×10^{-3} mmol, 1 equiv.) was azeotropically dried in vacuo with toluene followed by back purging with Argon for three times prior to use. Then dry DCM (1 mL) was added via syringe under Argon atmosphere to dissolve PEG_{10k}, followed by addition of ϵ -caprolactone (26.9 μ L, 0.23mmol, 57 equiv.) and MSA (0.8 μ L, 0.012 mmol, 3 equiv.) with stirring. After 2 hours, an aliquot of 10 μ L of the MI solution was taken for ¹H NMR and GPC analysis to check the monomer conversion, as exemplified in Fig. S1. Once the full conversion was confirmed, BOD (31.9 mg, 0.14mmol, 35 equiv.) was added to the macroinitiator solution with stirring. The rest procedures were same as those for preparing PEG/P(BOD) hydrogels.

To note the solid weight percentage in the hydrogel precursor solution for all the samples mentioned in this paper is kept at 10%.

Water capacity measurement

To measure the equilibrium swelling ratio (Q), the hydrogels were dehydrated by soaking in DEE for 1 hour, followed by drying in vacuo (60 °C, 20 mbar) for 24 hours. The weight of dry and fully swollen samples was determined by analytical balance and denoted as W_d and W_s , respectively, The equilibrium swelling ratio (Q) is defined as follows,

$$Q = \frac{W_s}{W_d}$$

The water content is calculated as $(W_s - W_d)/W_d$.

Mechanical tests

To obtain the compressive strain-stress curves, cylindrical hydrated hydrogel samples (diameter: 9mm; height: 8.5mm) were compressed to their maximum strain between two parallel plates at a crosshead speed of 0.1mm/second. Engineering stresses and strains were recorded.

For hysteresis and anti-fatigue measurements, the samples were first compressed to 60% strain at the rate of 0.1mm/second and then unloaded. After the samples restored to their original shapes, the samples were reloaded to the same strain level at the same speed as the first loading and unloaded again. The loading-unloading process was repeatedly conducted on the same samples for 5 cycles. Then the same samples were sequentially subject to 5 cycles of loading-unloading at the strain level of 70% and 80% operated in the same manner as at 60%.

The hysteresis energy was calculated using the equation as follows, where σ and ϵ represent compressive stress and strain, respectively.

$$U_{\text{hysteresis}} = \int_{\text{loading}} \sigma d\epsilon - \int_{\text{unloading}} \sigma d\epsilon$$

The recovery rate was quantified by comparing the hysteresis energy of subsequent cycles to that of the first cycle.

Drug loading

The dried hydrogel samples (~20 mg) were immersed in 10 mL of aqueous dispersion of DOX (4mg) with stirring. After the hydrogel samples reached equilibrium swelling, they were immersed in fresh water which was replaced every 12 hours, for further removal of unloaded free drugs. The unloaded drugs were collected via freeze-drying of aqueous dispersion and dissolved in THF. The amount of free drugs was determined by measuring the UV-Vis absorbance around 480 nm in THF using calibration curves generated from standard solutions. As such, drug loading capacity (DLC) of each hydrogel sample can be calculated as follows,

$$\text{DLC} = \frac{\text{Weigh of loaded drugs}}{\text{Weigh of dry hydrogel sample}}$$

In vitro drug release

The drug-loaded hydrogel samples were immersed in 6mL of PBS (pH=7.4) or PBS (pH=7.4) containing FBS (10 v/v %) with gentle shaking. At regular intervals, 2 mL of media was withdrawn and sampled for UV-Vis. The media was replenished with 2 mL of fresh solution. The release of DOX was determined according to calibration curve.

Hydrogel degradation study

Dehydrated hydrogels were weighed and placed into 20 mL of FBS-containing (10 v/v %) PBS solution (pH=7.4). The vials were capped and placed into a temperature controlled orbital shaker (37 °C, 100 rpm). The samples were removed from the orbital shaker at certain time point and washed in deionized water. Then the samples were re-dehydrated by soaking in ethanol for 1 hour followed by drying in vacuo (60 °C, 20 mbar) for 24 hours. Finally, the samples were weighed and the mass values obtained were plotted against time to obtain the degradation profiles.

Cell culture

HeLa cells were maintained in 'complete' DMEM (supplemented with 10% FBS, 1× GlutaMAX™, and 1× antibiotic-antimycotic) in a humidified atmosphere containing 5% CO₂ at 37 °C. Usually, cells were seeded in a T175 flask (ca. 3 × 10⁶ cells/mL) and passaged twice a week prior to the performance of the subsequent cell viability study.

Cytotoxicity assay

To assess the cytotoxicity of the hydrogels, dehydrated samples (~20 mg) were placed in an 80 v/v % ethanol solution for 1 hour, then washed with sterile PBS for 3 times, and finally incubated in sterile DMEM at 37 °C for 3 days, prior to the study.

The cells were cultured into a 24-well plate at a concentration of 2000 cells/well except for the 'medium blanks' in which the same amount of medium was added instead. Experimental wells received the sterilized hydrogel samples (or DOX-loaded hydrogel samples) and the plate was subsequently incubated in a humidified atmosphere containing 5 % CO₂ at 37°C. After certain period of time, 100 μL of alamarBlue® cell viability reagent (10% volume of cell culture media) was added to each well (except for three wells containing medium only). After 4 hours of incubation under the same growth conditions, the absorbance at 570 and 600 nm of each well was measured using a Varian Cary 50 Bio UV-Visible spectrophotometer. The absorbance of each

well was corrected against the medium-only wells without alamarBlue® reagent and then expressed as a percentage of the growth control.

Statistical analysis

The standard deviation was calculated from three samples in each study, presented as error bars in each plot.

Supplementary results and discussions

Table S1 Summary of the properties of the hydrogels

Sample ^a	EG/CL(PCL+BOD) molar ratio	Cross- linker (BOD) (w.t. %)	$\phi_{CL,0}$ ^b	ϕ_0 ^b	ϕ_{PEG} ^c	ϕ_{PCL} ^c	ϕ ^c	Q	Water Content (%)	Young's Modulus ^d (MPa)	Ultimate Stress (MPa)	Max. Strain (%)
PEG _{6k} /P(BOD)	88/12	25.3	0.022	0.081	0.048	0.018	0.066	13.03 ± 1.91	91.94	0.03 ± 0.0033	0.036 ± 0.0083	80.3 ± 4.83
PEG _{6k} /P(BOD)	78/22	41.7	0.036	0.082	0.21	0.16	0.37	2.43 ± 0.12	58.26	0.27 ± 0.052	1.98 ± 0.36	60.6 ± 3.15
PEG _{6k} /P(BOD)	64/36	59.5	0.052	0.084	0.20	0.33	0.53	1.75 ± 0.24	42.42	2.69 ± 0.27	3.26 ± 0.37	42.5 ± 2.94
PCL _{1.5k} -PEG _{6k} - PCL _{1.5k} /P(BOD)	64/36	36.6	0.052	0.084	0.13	0.21	0.34	2.63 ± 0.09	61.98	0.29 ± 0.0020	18.16 ± 3.73	98.1 ± 1.45
PCL _{3k} /PEG _{6k} /BOD	64/36	36.6	0.052	0.084	0.16	0.26	0.42	2.15 ± 0.06	53.50	1.34 ± 0.11	2.43 ± 0.18	51.7 ± 1.23
PEG _{10k} /P(BOD)	78/22	41.7	0.036	0.082	0.087	0.067	0.16	5.47± 0.34	81.72	0.04 ± 0.0061	0.35 ± 0.060	78.4 ± 4.55
PEG _{10k} /P(BOD)	64/36	59.5	0.052	0.084	0.13	0.21	0.35	2.57 ± 0.01	61.09	0.64 ± 0.13	2.68 ± 0.45	80.2 ± 4.94
PCL _{1.5k} -PEG _{10k} - PCL _{1.5k} /P(BOD)	64/36	46.0	0.052	0.084	0.13	0.21	0.33	2.77 ± 0.10	63.90	0.096 ± 0.010	29.37 ± 2.68	89.8 ± 2.96
PCL _{3k} -PEG _{10k} - PCL _{3k} /P(BOD)	64/36	32.0	0.052	0.084	0.12	0.19	0.31	2.89 ± 0.04	65.40	0.18 ± 0.0020	31.41 ± 2.50	97.4 ± 1.21
PEG	100/0	-	0	0.079	0.031	0	0.031	25.8 ± 1.11	96.12	0.01 ± 0.0012	0.035 ± 0.0081	61.1 ± 2.52

^a PCL-PEG-PCL/P(BOD) refers to the architecture shown in Scheme 1 (a) (main text); PEG/P(BOD) refers to Scheme 1 (b); PCL/PEG/P(BOD) Scheme 1 (c).

^b $\phi_{CL,0}$ is the initial volume fraction of CL units and ϕ_0 is the total initial volume fraction. $\phi_0 = \phi_{PEG,0} + \phi_{CL,0}$.

ϕ_0 was kept around 0.08 in order to minimize the effect of initial volume of constituents on the properties of the hydrogels.³ The initial solid weight percentage for all the hydrogel samples discussed herein is 10%.

^c ϕ_{PEG} and ϕ_{PCL} is the volume fraction of PEG and PCL components in the swollen hydrogel, respectively. ϕ is the total polymer volume fraction in the hydrated matrix. $\phi = \phi_{PEG} + \phi_{PCL}$. The lower ϕ is, the more water the hydrogel can retain. Also, it should be noted that, 100% cross-linker conversion was assumed for all calculations, based on the prior report.⁴

^d Young's modulus is calculated as the slope of initial linear region (5% - 10% strain) of compressive strain-stress curve.

Table S2 Molecular weight of linear polymers involved in the preparation of hydrogel networks

Polymers ^a	M_n^{NMR} (kDa) ^b	M_n^{GPC} (kDa) ^c	PDI ^c
PEG _{6k}	-	6.0	1.02
PEG _{10k}	-	10.0	1.03
PCL _{3k}	3.4	3.3	1.05

PCL _{1.5k} -PEG _{6k} -PCL _{1.5k}	9.4	9.2	1.03
PCL _{1.5k} -PEG _{10k} -PCL _{1.5k}	13.4	13.0	1.03
PCL _{3k} -PEG _{10k} -PCL _{3k}	16.8	16.7	1.02

^a PEG_{6k} and PEG_{10k} are purchased and used after azeotropically dried in vacuo with toluene. The rest linear polymers were synthesized via ROP.

^b M_n was calculated given 100% conversion of CL according to ¹H NMR.

^c M_n and PDI were determined by THF GPC, using calibration curve.

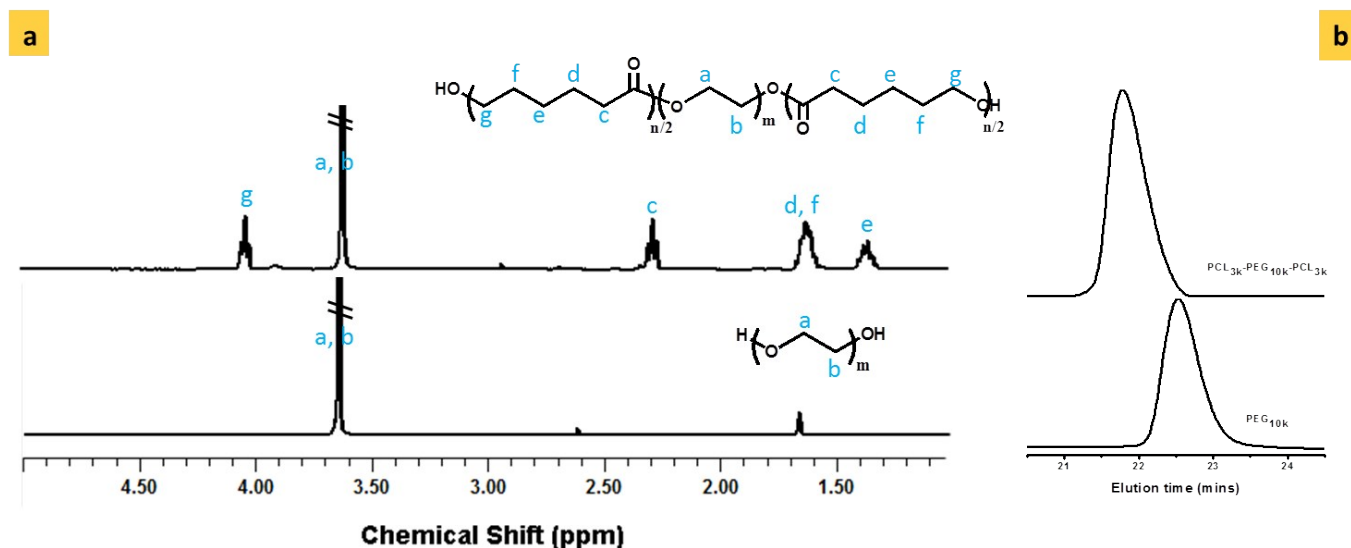


Fig. S1 Characterizations of a PCL-PEG-PCL triblock linear polymer (PCL_{3k}-PEG_{10k}-PCL_{3k}) and initiator (PEG_{10k}) involved in the hydrogel preparation: **(a)** ¹H NMR spectrum (in CDCl₃) **(b)** THF GPC differential refractive index (DRI) chromatograms

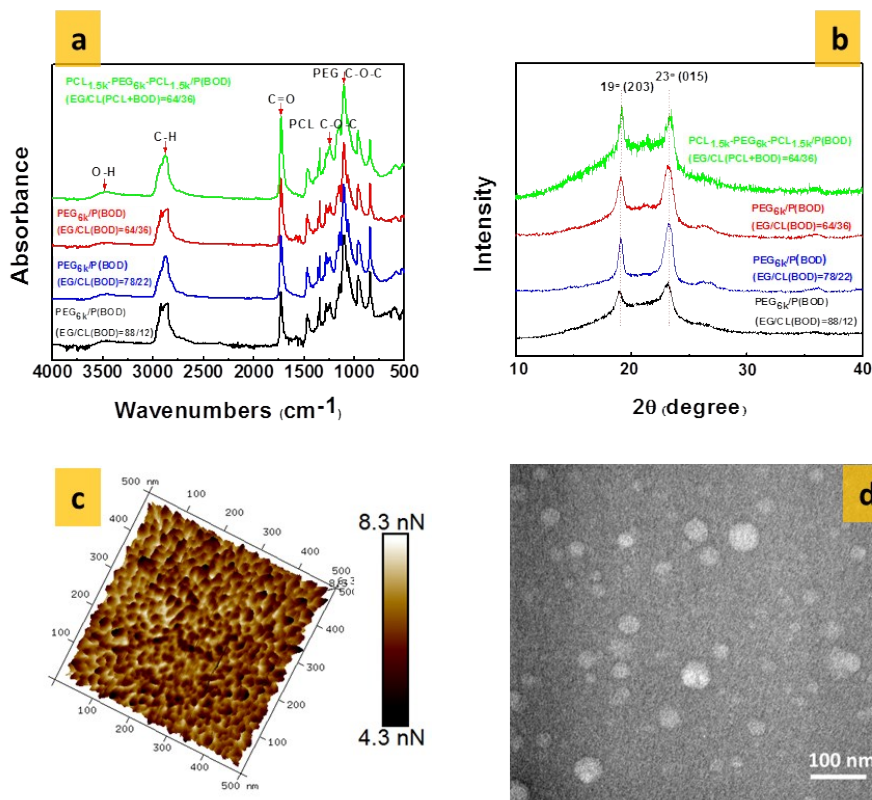


Fig. S2 (a) ATR-IR spectra **(b)** XRD pattern of hydrogels with different compositions (EG/CL molar ratios); **(c)** AFM 3-D adhesion mapping contour plot of spin-coated PCL-PEG-PCL/P(BOD) hydrogel film for characterization of hydrophobic domains; **(d)** TEM image of PCL-PEG-PCL/P(BOD) hydrogel film prepared by FIB to further confirm the presence of hydrophobic domains in the matrix

In the spectrum (Fig. S2a, ESI[†]), absorption bands around 1103 and 1243 cm^{-1} are attributed to C-O-C stretching vibration of PEG and PCL backbones, respectively. The relative intensity of the PCL band to that of PEG increases as the CL content is increased (Table S2, ESI[†]), indicating the formation of PCL segments during the gelation. The evident peak at 1726 cm^{-1} , corresponding to the C=O stretch of the ester carbonyl group, is also indicative of the incorporation of PCL chains. The addition of the CL results in the increase in the relative intensity of this band to the PEG-related band. The signals of C-H and O-H stretch can be seen in the broad bands within 2800-3000 and 3100-3500 cm^{-1} , respectively. Together, the bands observed in the ATR-IR spectra verify the successful crosslinking of PEG and PCL moieties through ester linkages.

Table S3 Relative intensity of characteristic bands of PEG to those of PCL moieties

Hydrogels	EG/CL (PCL+BOD) molar ratio	PCL C-O-C /PEG C-O-C	C=O /PEG C-O-C
PEG _{6k} /P(BOD)	88/12	0.395	0.502
PEG _{6k} /P(BOD)	78/22	0.417	0.571
PEG _{6k} /P(BOD)	64/36	0.458	0.685
PCL _{1.5k} -PEG _{6k} -PCL _{1.5k} /P(BOD)	64/36	0.489	0.724

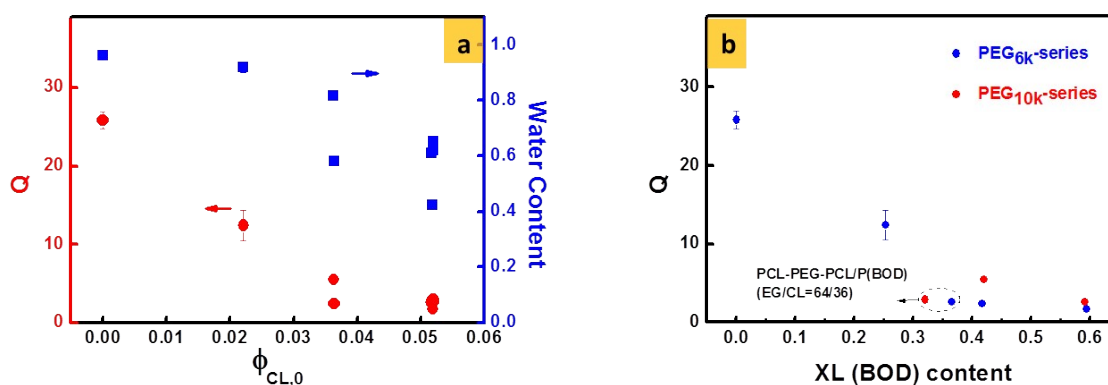


Fig. S3 (a) Equilibrium swelling ratio (Q) and water content as a function of initial volume fraction CL units ($\phi_{CL,0}$) **(b)** Q as a function of cross-linker(XL) BOD content: the circled data points refer to the PCL-PEG-PCL/BOD hydrogels prepared from the same infeed EG/CL(PCL+BOD) molar ratio (64/36) yet lower XL content, compared with the PEG/P(BOD) counterparts in the far right of the graph

The equilibrium swelling ratio (Q) and water retention of the hydrogels could be tuned by varying their hydrophilic/hydrophobic balance that was controlled by the initial volume fraction of PEG ($\phi_{PEG,0}$) and CL ($\phi_{CL,0}$). The total initial volume fraction (ϕ_0) of PEG and CL was fixed for all hydrogels. As expected, the introduction of hydrophobic CL content significantly reduces the water capacity of these hydrogels, as shown in the Fig. S3a, ESI[†], where Q falls from 25.8 to 1.74 and water content from 96.1% to 42.4%, with increase in the $\phi_{CL,0}$. It appears that the states of converted CL, whether it be from ϵ -caprolactone monomers or BOD cross-linker, have little influence on the swelling capacity of the hydrogels. In the case of the PCL-PEG-PCL/P(BOD) hydrogels with $\phi_{CL,0}$ of 0.052, where more ϵ -caprolactone monomers were added in place of BOD cross-linker while $\phi_{CL,0}$ was held constant, the Q value is still close to that of the other PEG/P(BOD) hydrogels prepared with the same $\phi_{CL,0}$ (Fig. S3b,

ESI⁺). Fig. S3b, ESI⁺ also displays the effect of PEG chain length on the swelling of the hydrogels, with Q values increased as PEG chain was extended from 6k to 10k, all other parameters being equal.

Table S4 Compressive mechanical properties of different kinds of tough hydrogels

Hydrogels	Initial solid (w.t.%)	Swelling	Modulus (kPa)	Ultimate Stress (MPa)	Max. Strain (%)	Toughness (kJ/m ³)	Ref
PAMPS/PAAm DN interpenetrated with PEDOT	-	6	162	10.5	98	18	5
Alginate/PEGMA DN	86	3.1	350	0.5	70	70	6
Agar/PAAm DN	~21	-	123	38	94	9000	7
Silicon/PHEA interpenetrating network	~45	-	-	21	98	6500	8
PEGDA-Laponite composite	10	5.8	37.9	3.8	95.0	254	9
PAAm-Laponite-Dopamine composite	~11	4	275	4.4	~100	950	10
PAAm- hydroxyapatite composite	~12	4	90	35	95	-	11
Tetra-armed PEG network	~12	~1	-	60	~100	-	12
PEG diacrylate network with hydrophobic side chain oligo(trimethylene carbonate)	10	42.6	14.9	5.2	98.2	215	13
PCL _{3k} -PEG _{10k} -PCL _{3k} /P(BOD)	10	2.9	184	31.4	97.4	2794	This work

PAAm: poly(acrylamide)

PEDOT: poly(3,4-ethylenedioxythiophene)

PEGMA: poly(ethylene glycol) methyl ether methacrylate

PHEA: poly(hydroxyethyl) acrylate

PEGDA: poly(ethylene glycol) diacrylate

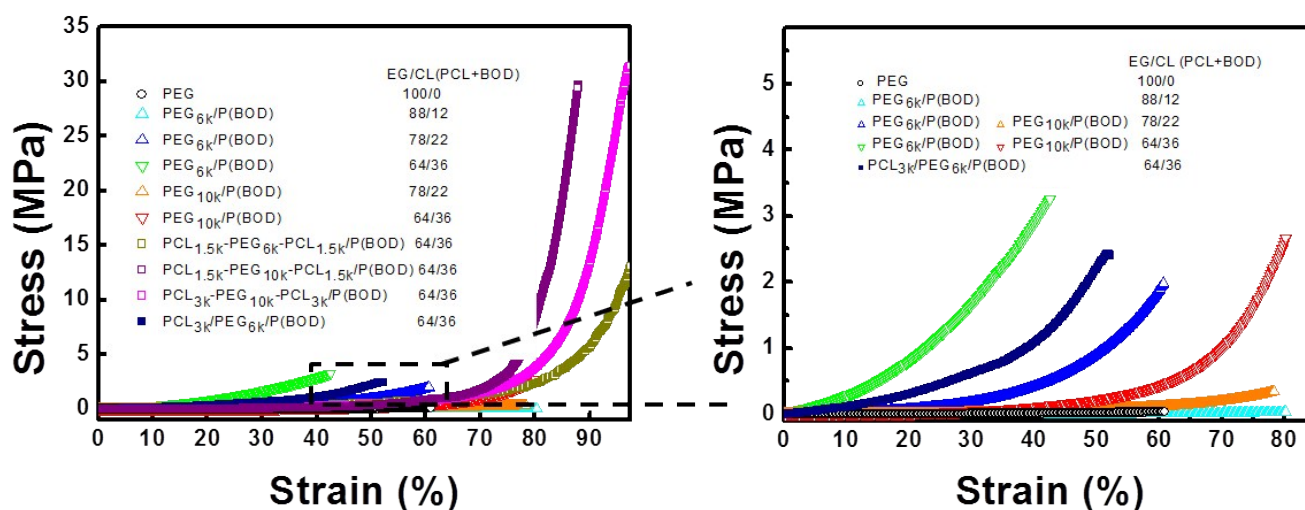


Fig. S4 Compressive curve summary of all the hydrogels with different compositions and architectures. Magnified part highlights the compressive curves of PEG/P(BOD) and PCL/PEG/P(BOD) hydrogels

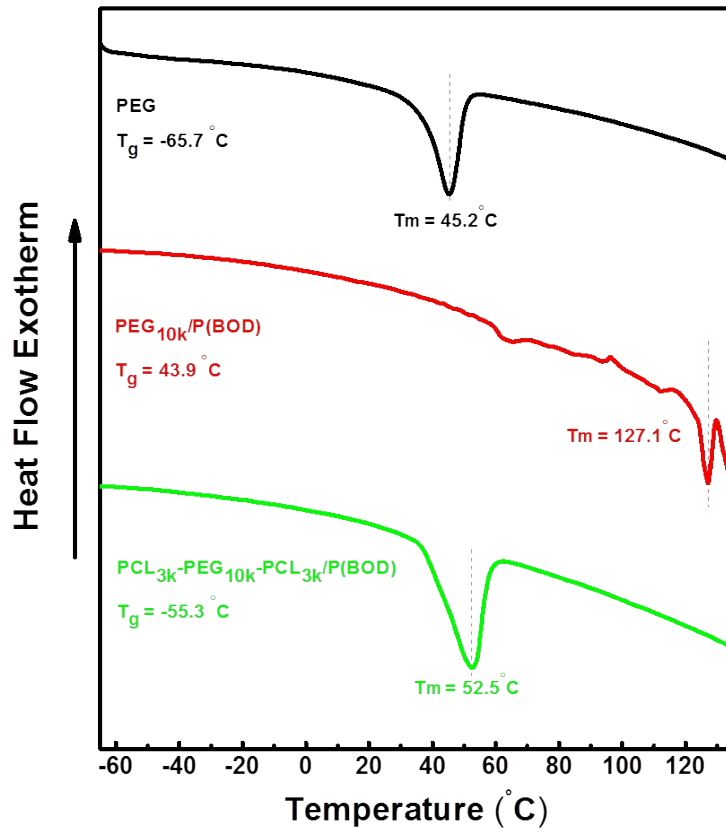


Fig. S5 DSC thermograms of PEG, PEG_{10k}/P(BOD) (EG/CL(BOD)=64/36) and PCL_{3k}-PEG_{10k}-PCL_{3k}/P(BOD) (EG/CL(PCL+BOD)=64/36) hydrogels

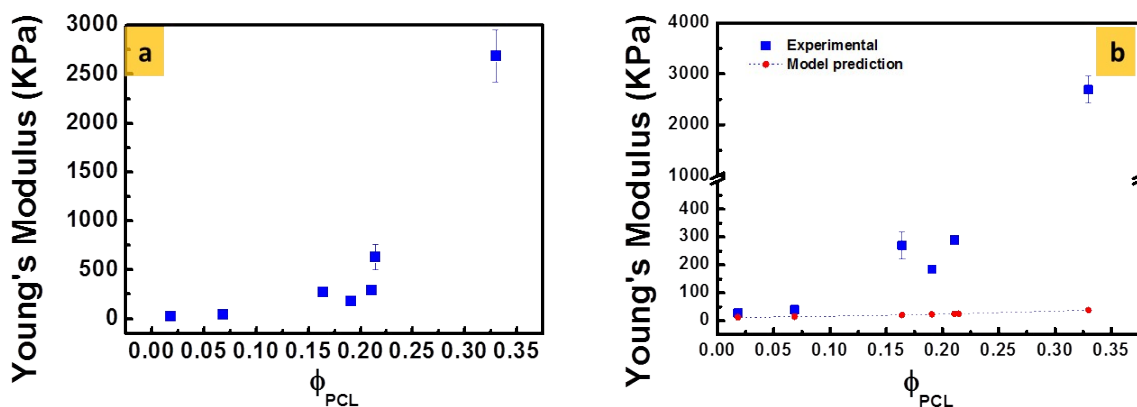


Fig. S6 (a) Young's Modulus as a function of equilibrium volume fraction of PCL components (ϕ_{PCL}); (b) Experimental Young's modulus (E) as a function of the equilibrium volume fraction of PCL (ϕ_{PCL}) in the fully swollen hydrogels (blue squares) vs. the theoretical values (red circles along a dashed line) predicted by the Guth-Gold model ($E = E_0(1 + 2.5\phi_{particle} + 14.1\phi_{particle}^2)$); E_0 is the Young's modulus of PEG hydrogel and $\phi_{particle}$ is the volume fraction of rigid fillers)

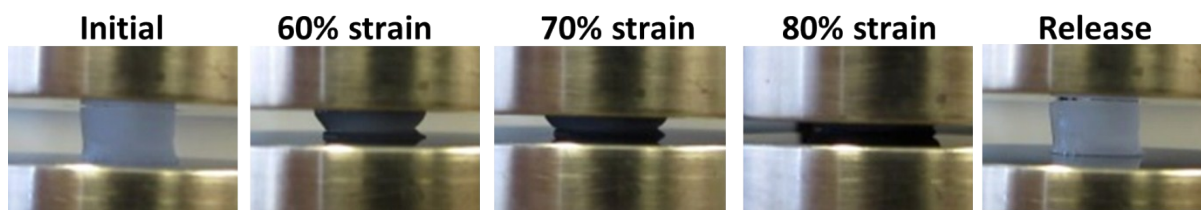


Fig. S7 Photographs showing recovery of the PCL-PEG-PCL/P(BOD) (EG/CL(PCL+BOD)=64/36) hydrogel to its original shape after undergoing a series of compressive loading at different strain levels

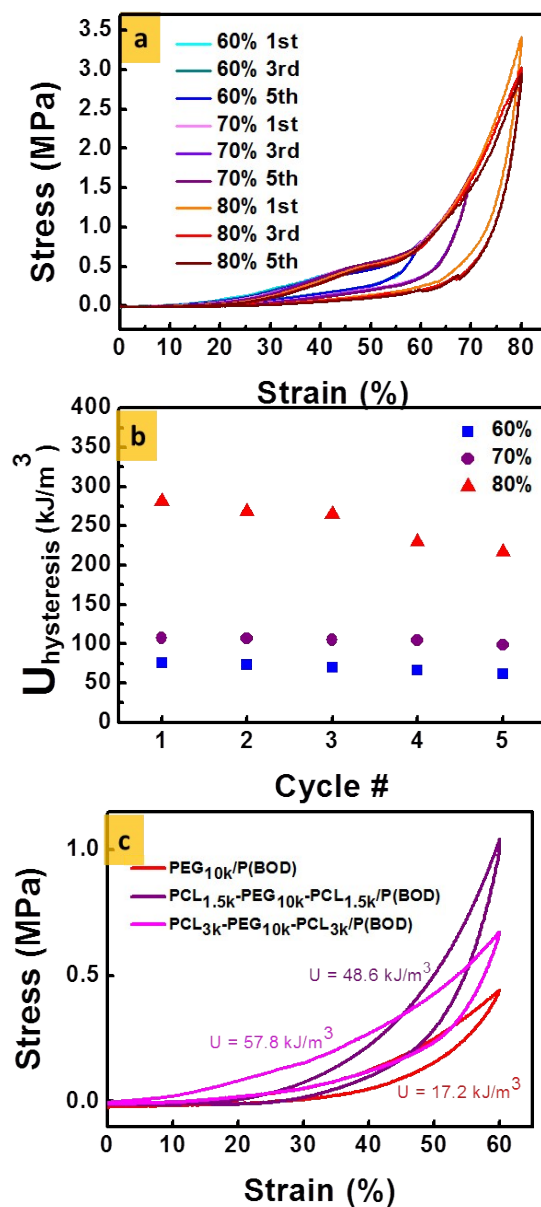


Fig. S8 (a) Successive loading-unloading curves of PCL_{3k}-PEG_{10k}-PCL_{3k}/P(BOD)

(EG/CL(PCL+BOD)=64/36) hydrogels at the strain of 60%, 70% and 80% **(b)** Hysteresis energy of loading-unloading cycles at different strains as a function of the nummber of cycle **(c)** Hysteresis (at the same strain 60%) comparison among PEG_{10k}/P(BOD), PCL_{1.5k}-PEG_{10k}-PCL_{1.5k}/P(BOD) and PCL_{3k}-PEG_{10k}-PCL_{3k}/P(BOD), with the same infeed EG/CL molar ratio (64/36) but different content of linear PCL segments

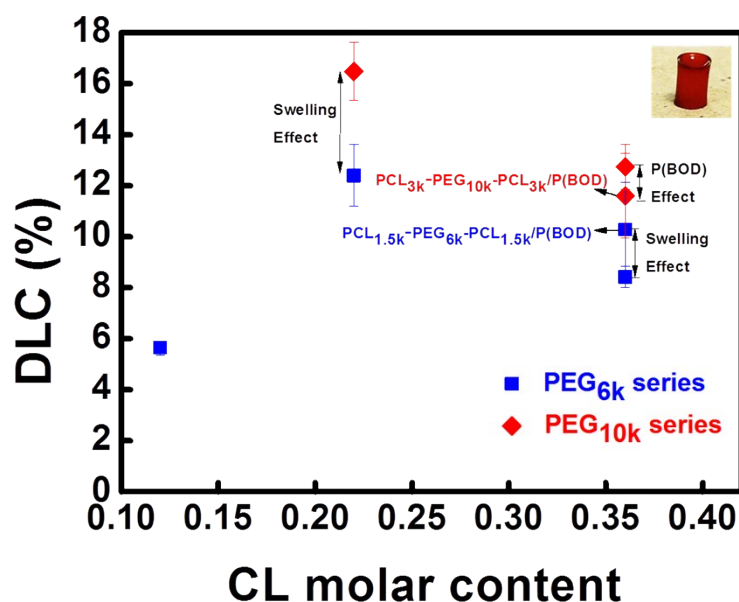


Fig. S9 Drug loading capacity (DLC) of the hydrogels with different compositions as a function of infeed CL molar content: DLC is determined by combined effect of hydrophobic content (particularly P(BOD)) and swelling ratio; inserted photograph shows an example of a DOX-loaded hydrogel

Table S5 Summary of DLC of the hydrogels with different compositions

Hydrogels	EG/CL(PCL+BOD) ratio	Drug Loading Capacity (DLC, %)
PEG _{6k} /P(BOD)	88/12	5.4 ± 0.3
PEG _{6k} /P(BOD)	78/22	11.5 ± 1.2
PEG _{6k} /P(BOD)	64/36	8.7 ± 0.4
PCL _{1.5k} -PEG _{6k} -PCL _{1.5k} /P(BOD)	64/36	9.0 ± 1.9
PEG _{10k} /P(BOD)	78/22	17.3 ± 1.1
PEG _{10k} /P(BOD)	64/36	12.1 ± 0.9
PCL _{3k} -PEG _{10k} -PCL _{3k} /P(BOD)	64/36	10.4 ± 1.7

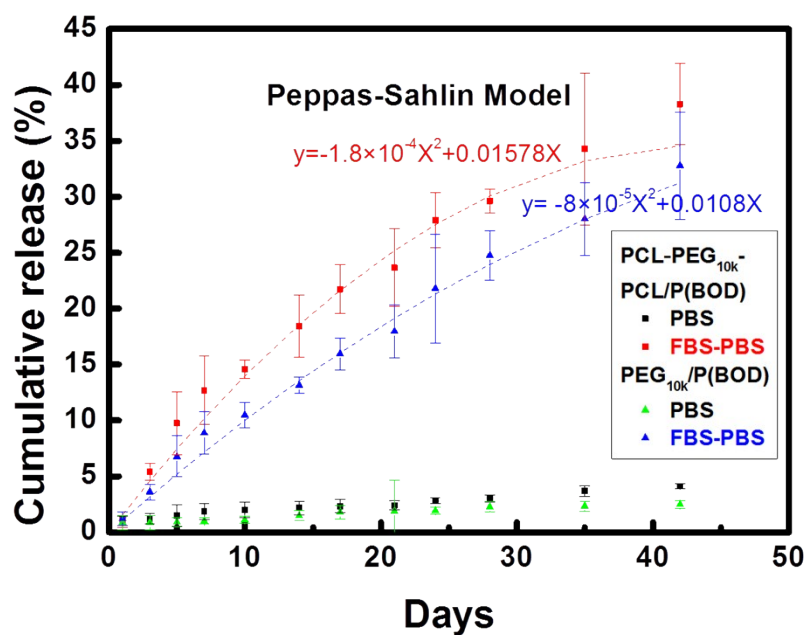


Fig. S10 Release profile of PCL_{3k}-PEG_{10k}-PCL_{3k}/P(BOD) and PEG_{10k}/P(BOD) hydrogels prepared from the same infeed EG/CL molar ratio under neutral PBS (pH=7.4) and FBS-containing (10 v/v %) PBS (pH=7.4) over 6 weeks; the release profile can be fitted to Peppas - Sahlin model, with the equation presented in the figure

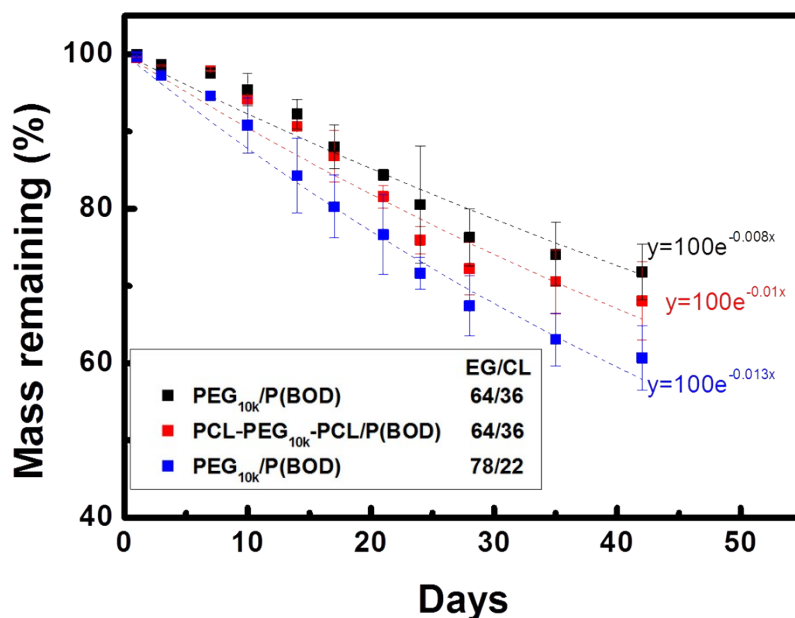


Fig. S11 Degradation profile of PCL_{3k}-PEG_{10k}-PCL_{3k}/P(BOD) and PEG_{10k}/P(BOD) hydrogels with different compositions under the condition of FBS-containing (10 v/v %) PBS (pH=7.4) over 6 weeks; the mass degradation profile can be fitted to pseudo-first order model ($\frac{dm}{dt} = -km$), with the equation presented; the

faster degradation with lower PCL content was observed, arising from the increased swelling of the hydrogel as a result of less hydrophobic components

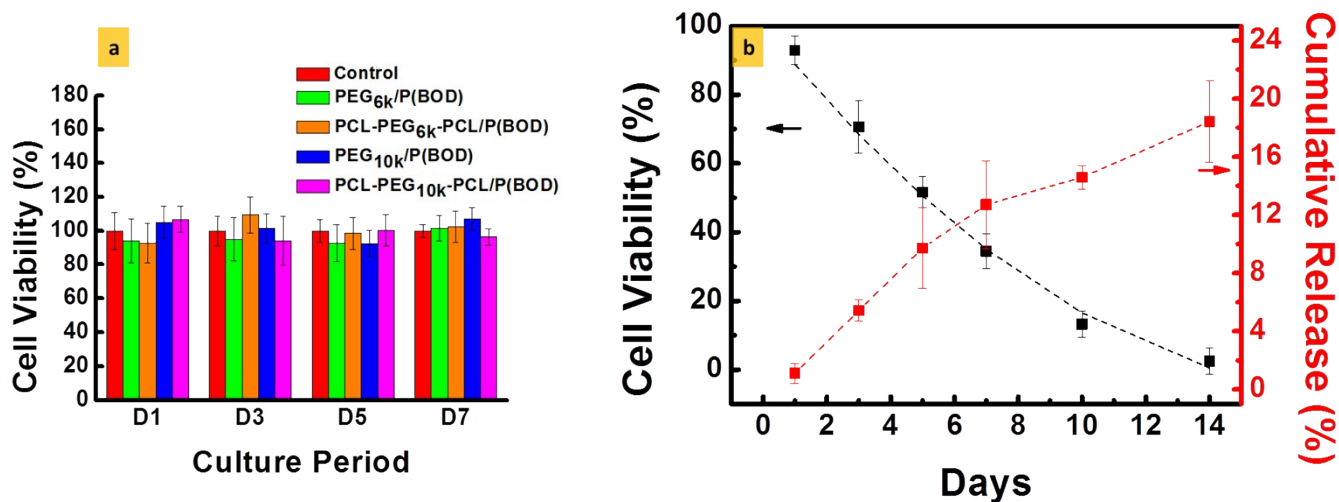


Fig. S12 (a) Cytotoxicity of various hydrogels to HeLa cells during 1 week; (b) viability of HeLa cells upon exposure to DOX-loaded PCL_{3k}-PEG_{10k}-PCL_{3k}/P(BOD) hydrogels for 2 weeks, vs. release profile of the DOX-loaded PCL_{3k}-PEG_{10k}-PCL_{3k}/P(BOD) hydrogels in FBS-containing PBS solution (10 v/v %, pH=7.4) over the same period

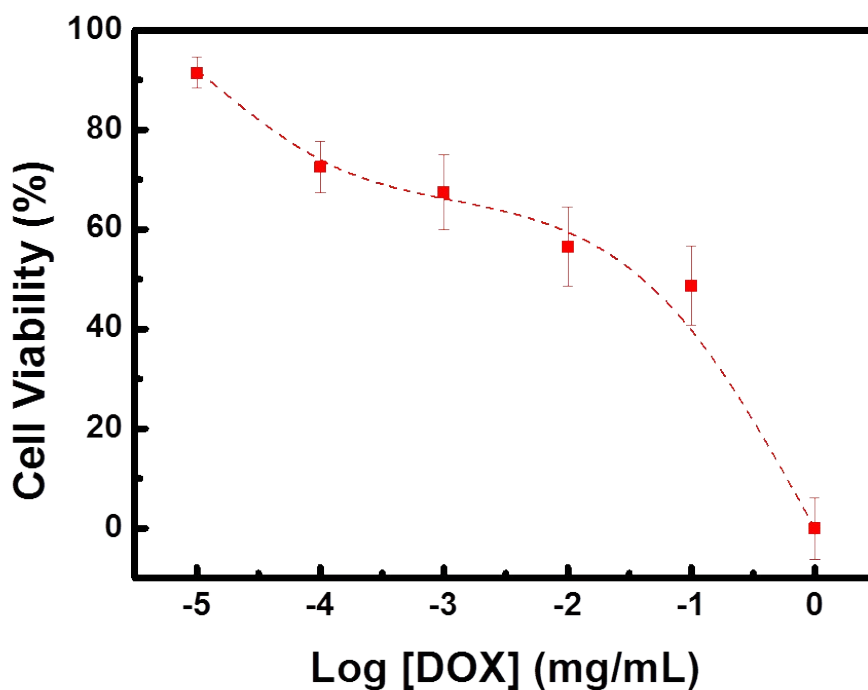


Fig. S13 Viability of HeLa cells upon exposure to free DOX at different concentrations, used as a reference to estimate the concentration of released DOX from the hydrogel carrier in the cell solution

References

1. B. Ozcelik, K. D. Brown, A. Blencowe, et al., *Advanced healthcare materials*, 2014, **3**, 1496-1507.
2. J. T. Wiltshire and G. G. Qiao, *Macromolecules*, 2006, **39**, 4282-4285.
3. J. Cui, M. A. Lackey, G. N. Tew, et al., *Macromolecules*, 2012, **45**, 6104-6110.
4. D. Gu, K. Ladewig, M. Klimak, et al., *Polymer Chemistry*, 2015, **6**, 6475-6487.
5. G. Du, G. Gao, R. Hou, et al., *Chemistry of Materials*, 2014, **26**, 3522-3529.
6. Z. W. Low, P. L. Chee, D. Kai, et al., *Rsc Advances*, 2015, **5**, 57678-57685.
7. Q. Chen, L. Zhu, C. Zhao, et al., *Advanced materials*, 2013, **25**, 4171-4176.
8. L. Si, X. Zheng, J. Nie, et al., *Chemical Communications*, 2016, **52**, 8365-8368.
9. C. W. Chang, A. van Spreeuwel, C. Zhang, et al., *Soft Matter*, 2010, **6**, 5157-5164.
10. S. Skelton, M. Bostwick, K. O'Connor, et al., *Soft Matter*, 2013, **9**, 3825-3833.
11. Z. Y. Li, Y. L. Su, B. Q. Xie, et al., *Journal of Materials Chemistry B*, 2013, **1**, 1755-1764.
12. H. Kamata, Y. Akagi, Y. Kayasuga-Kariya, et al., *Science*, 2014, **343**, 873-875.
13. C. Zhang, A. Aung, L. Q. Liao, et al., *Soft Matter*, 2009, **5**, 3831-3834.